Vacancy effect on the doping of silicon nanowires: A first-principles study*

Liu Yang(刘 阳)[a], Liang Pei(梁 培)[a)c)†], Shu Hai-Bo(舒海波)[a], Cao Dan(曹 丹)[b], Dong Qian-Min(董前民)[a], and Wang Le(王 乐)[a]

[a] College of Optical and Electronic Technology, China Jiliang University, Hangzhou 310018, China
[b] College of Science, China Jiliang University, Hangzhou 310018, China
[c] Department of Physics, South China University of Technology, Guangzhou 510640, China

(Received 26 September 2013; revised manuscript received 5 December 2013; published online 20 April 2014)

The influence of vacancy defect on the doping of silicon nanowires is systematically studied by the first-principles calculations. The atomic structures and electronic properties of vacancies and vacancy–boron (vacancy–phosphor) complexes in H-passivated silicon nanowire with a diameter of 2.3 nm are explored. The results of geometry optimization indicate that a central vacancy can exist stably, while the vacancy at the edge of the nanowire undergoes a local surface reconstruction, which results in the extradition of the vacancy out of the nanowire. Total-energy calculations indicate that the central vacancy tends to form a vacancy–dopant defect pair. Further analysis shows that n-type doping efficiency is strongly inhibited by the unintentional vacancy defect. In contrast, the vacancy defect has little effect on p-type doping. Our results suggest that the vacancy defect should be avoided during the growth and the fabrication of devices.

Keywords: silicon nanowire, vacancy, doping, density-functional theory

PACS: 73.20.Hb, 73.21.Hb, 71.15.Mb **DOI:** 10.1088/1674-1056/23/6/067304

1. Introduction

Silicon-based materials are among the most researched materials in the semiconductor field, especially the integrated circuit (IC) field. The nano-scaled material exhibits intriguing electronic and optical properties due to the quantum size effect, which attracts a great deal of scientific and technological attention.[1–3] One-dimensional silicon nanowires (SiNWs) are regarded as one of the most important nanomaterials due to many potential applications, such as field-effect transistors,[4] solar cells,[5,6] chemical and biological sensors.[7,8] The realization of these applications depends on fabricating high-quality SiNWs with a special size, shape, doping type, and stability in the process of use.

To realize the applications of SiNWs in nano-devices, many methods have been developed to prepare high-quality SiNWs,[9,10] such as metal-catalytic vapor–liquid–solid, oxide-assisted method, and the solution method. Experimentally, [110] direction is a major growth direction in small diameter SiNWs. While the SiNWs with the [111] and [112] directions are preferred in the larger size.[10] In addition to the synthesis of high-quality SiNWs, the realization of SiNWs in nano-devices, in particular the nano-electronic devices, requires sufficiently high carrier concentrations to ensure the performance of devices. Doping is regarded as an important way to obtain free carriers. However, the doping efficiency of SiNWs is lower than what we expected, in particular for n-type doping. For instance, Cui *et al.*[11] reported on the preparation of the n-type and p-type SiNWs by doping P and B atoms, respectively. Although n-type SiNWs were successfully realized, the carrier concentration of P-doped NWs was far lower than that of B-doped NWs using the same level of doping concentrations.[12,13] The mechanism for the P-doped SiNWs with the low carrier concentration is still unclear. Unintentional defects, such as vacancy point defects and surface dangling bonds, are possible to produce in nanomaterials. Therefore, it is important to understand the effects of vacancy and surface dangling bonds on the doping properties of SiNWs.

In the past, both experimental and theoretical studies have reported on the effect of the surface dangling bond on the electronic properties of SiNWs. For example, Hong *et al.*[14] performed a first-principles calculation to investigate the effect of the surface dangling bond on the doping of SiNW. Their results showed that the surface dangling bond is a fundamental obstacle for the doping of SiNWs. Peelaers *et al.*[15] reported that the surface dangling bond traps the phosphor dopant, resulting in lower conductance. For the vacancy point defects, there have been few reports till now. Ko *et al.*[16] performed a tight-binding Green function approach to investigate the electronic properties of SiNWs with different defects, such as vacancies, substitutional defects, and surface dangling bonds. They found a low electrical conductivity in SiNWs with these different defects. Nevertheless, the mechanism of the vacancy

*Project supported by the National Natural Science Foundation of China (Grant Nos. 61006051 and 61177050) and the Zhejiang Provincial Natural Science Foundation, China (Grant No. Y1110777).

†Corresponding author. E-mail: plianghust@126.com

© 2014 Chinese Physical Society and IOP Publishing Ltd

effect on the electronic properties of SiNWs has not been clarified.

In this work, we report on a systematic investigation for the effects of unintentional vacancy defects on the electronic and the doping properties of SiNWs by using the first-principles calculations. The stability of various unintentional vacancy defects and defect complexes, and the effects of vacancy defects on the n- and p-type-doped SiNWs are studied in detail. We expect that our study can contribute to the improvement of doping processing of SiNWs in experiment.

2. Details and methods of calculations

All calculations in the present study are carried out within the density function theory as implemented in the Vienna *ab initio* simulation package (VASP).[17] The exchange–correlation energy is treated in the generalized-gradient approximation (GGA) with the Perdew–Burke–Ernzerhof (PBE)[18] functional, and the electron–ion interaction is described in the projector augmented wave (PAW) potential. The energy cutoff for the plane-wave expansion is set to 350 eV. In the geometry optimizations, all atoms are relaxed until the Hellman–Feynman force acting on each atom is less than 0.001 eV/Å.

The SiNWs are created on the basis of the optimized bulk Si structure. Thus, the lattice parameters of bulk Si are optimized first by using the Monkhorst–Pack sample with a $10 \times 10 \times 10$ k-points mesh, and the optimized lattice parameter is 5.485 Å that is 1% error in the experimental value. Then an SiNW with a diameter of 2.3 nm is extracted from the relaxed bulk Si along the [110] direction (see Fig. 1). To avoid the influence of surface dangling bonds, surface atoms of the nanowire are passivated by H atoms. The SiNW with a hexagonal cross section contains 216 atoms including 160 Si atoms and 56 H atoms. In the calculations of SiNWs, the Monkhorst–Pack k-point mesh of $1 \times 1 \times 10$ is found to provide sufficient accuracy in the Brillouin-zone integration. The distance between two neighboring SiNWs is larger than 10 Å to eliminate their interactions.

3. Results and discussion

3.1. Vacancy point defects in SiNWs

To investigate the vacancy effect on the doping of silicon nanowires, the properties of vacancy point defects in the nanowire need to be clarified first. A vacancy defect is formed by removing an Si atom from the nanowire. We consider two different vacancy configurations: one is located at the center of the wire (denoted as V_c) and the other lies at the edge of the wire (denoted as V_e). Both vacancy configurations undergo a local structural distortion after structural relaxation. For the V_c configuration (see Fig. 1(b)), two nearest neighboring Si atoms around the vacancy (radial Si atoms) approach each other due to the interaction between unpaired electrons. Their distance changes from 3.867 Å to 2.863 Å after structural relaxation. The other two Si atoms around the vacancy along the axial direction (axial Si atoms) are far from each other, and the distance of two Si atoms is 5.323 Å. For the V_e configuration (see Fig. 1(c)), the optimized result shows that the distance between the radial Si atoms around the vacancy is 2.497 Å, which is very close to the length of Si–Si bond (2.375 Å) and the axial Si atoms are far from each other. Owing to the bonding interaction between two Si atoms along the radial directions, the Si vacancy in the V_e configuration is forced out of the SiNW after the structural relaxation.

Figures 1(d)–1(f) show the band structures of SiNWs without and with Si vacancy, respectively. It is found that the perfect SiNW shows a direct band-gap feature (1.12 eV) with both the valence band maximum (VBM) and the conduction band minimum (CBM) at Γ point (see Fig. 1(d)), which is different from bulk Si of indirect band gap. In contrast, there are two localized defect levels in the gap for the V_c configuration (see Fig. 1(e)). The lower occupied level is close to VBM and the higher unoccupied level is 0.25 eV lower than CBM. The deep localized level may become a recombination center which induces the deduction of carrier concentration. In other words, free carriers can be captured by Si vacancies. For the V_e configuration, its band structure is similar to that of perfect SiNW. The possible reason is that the Si vacancy is removed from the nanowire and the dangling bonds of the neigboring Si atoms around the Si vacancy are passivated due to the surface reconstruction, thus the defect levels in the V_e configuration are close to the VBM/CBM.

To gain an insight into the origins of band-edge states and defect levels in SiNW without (with) vacancy, we plot the spatial distributions of charge-density in Fig. 2. The charge-density is plotted in three types, i.e., (a) VBM and CBM at the Γ point in the perfect SiNW, (b) two localized defect levels in the V_c configuration, and (c) VBM and CBM at the Γ point in the V_e configuration. The calculated charge-densities show that both VBM and CBM in the perfect SiNW and the V_e configuration localized at the core region of the nanowire (see Figs. 2(a) and 2(c)), indicating the electron excitation mainly from the core atoms. For the V_c configuration, it is found that the lower occupied level originates from the contribution of the neighboring Si atom around the vacancy, while the higher unoccupied level is derived mainly from the extended electronic states of Si atoms along the y-axis direction of vacancy. Therefore, the Si vacancy located at the center of SiNW will induce a deep defect level and the vacancy at the edge of the nanowire has little effect on the electronic structure of SiNW.

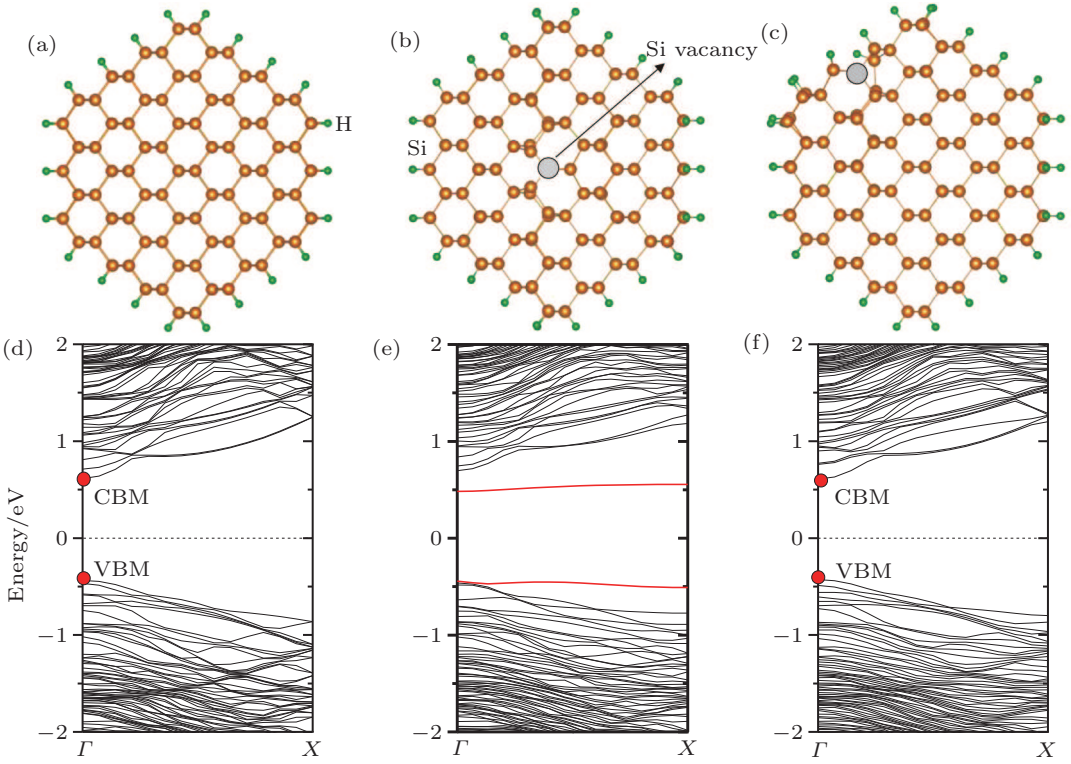


Fig. 1. (color online) Atomic structures and band structures of H-passivated Si nanowire without (with) vacancy. Panels (a)–(c) indicate the cross-section atomic structures of perfect SiNW, SiNW with a central Si vacancy, and SiNW with an Si vacancy at the edge of wire, respectively. Small size, medium size, and large size balls denote H atoms, Si atoms, and Si vacancy, respectively. Panels (d)–(f) show the band structures of perfect SiNW, SiNW with a central Si vacancy, and SiNW with an Si vacancy at the edge of the wire, respectively. The Fermi level is set to 0 eV.

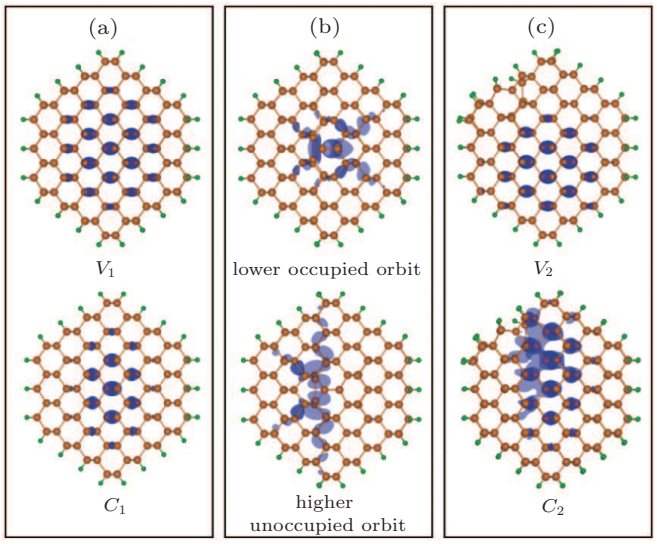


Fig. 2. (color online) Spatial distributions of charge-density in three configurations: (a) perfect SiNWs, (b) vacancy at the center of nanowire (V_c), and (c) vacancy at the edge of nanowire (V_e). V_i and C_i ($i = 1, 2$) represent VBM and CBM states at Γ point, respectively.

Because V_c can exist stably, while the V_e might be extruded out of SiNW due to the surface reconstruction, we only consider the V_c configuration. As is well known, the silicon atom has four outer shell electrons, so when one silicon atom is removed from the nanowire, the defective nanowire might not be electrically neutral. Here we consider different possible charged configurations to ascertain which charged state is the most stable one. The total energies of the V_c configuration with different values of charge q ($q = -2, -1, 0, +1, +2$) are calculated after all different cases have been reoptimized. For charged defect, the jellium background[19] is used. The formation energy (E_q)[20] of a vacancy configuration with charge q is defined as the function of the electron Fermi level E_F:

$$E_q = E_{tot} - E_{SiNWs} + \mu_{Si}^{bulk} + qE_F,$$

where E_{tot} and E_{SiNWs} represent the total energies of the supercell with a charged vacancy and free-vacancy, respectively,

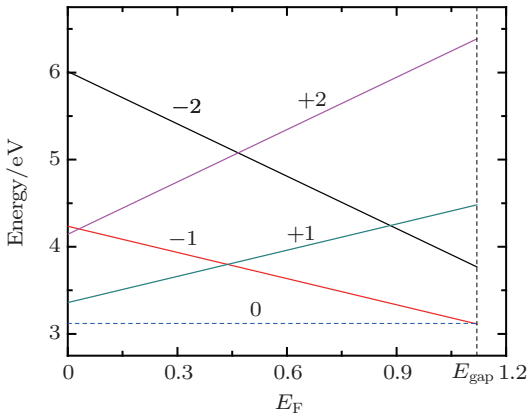


Fig. 3. (color online) Formation energies of vacancy in 2.3-nm diameter SiNWs with respect to the Fermi level. The numbers +2, +1, 0, −1, and +1 represent the positively charged, neutral, and negatively charged V_c configurations, respectively.

μ_{Si}^{bulk} is the total energy per atom of bulk Si, E_F is the Fermi level with respect to VBM of perfect SiNW. According to our results, it is obvious that the neutral case has the lowest formation energy in all the cases, expect for a small region near E_{gap}, meaning that the neutral case is the energetically favorable one (see Fig. 3). So the following calculations are based on neutral cases.

3.2. Vacancy effect on the doping of Si nanowires

We now come to investigate the effect of vacancy on the doping of SiNWs. The dopant atoms (B and P) are introduced into the V_c and V_e configurations, respectively. For the V_c configuration, three substitution sites (A, B, and C) are considered as shown in Fig. 4(a). A and B represent two neighboring substitution sites of vacancy and the C site is far from the Si vacancy. Similarly, three substitution sites are also considered in the V_e configuration. As shown in Fig. 4(b), A site is located at the center of the nanowire, B and C sites lie at two edges of the nanowire, respectively. The most stable doping site is obtained by comparing the total energies of doping configurations. Taking the lowest total energy among the doping configurations as energy zero, the total energy differences in the V_c and V_e configurations are listed in Table 1. The preferential positions of B and P dopants are B and A sites in the V_c configuration, respectively. The result suggests that the central Si vacancy can trap the dopant atoms to form vacancy-B or vacancy-P complexes. In contrast, the C and B sites are energetically favorable for the B-doped and P-doped nanowires in the V_e configuration, respectively. Therefore, the edge Si vacancy has no effect on trapping the dopant atoms, in particular the p-type dopants (e.g. B).

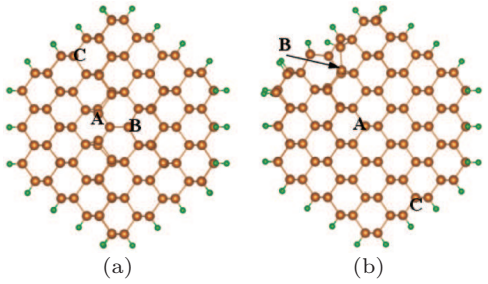


Fig. 4. (color online) Top view of atomic structures of B- (P)-doped H-passivated SiNWs with a vacancy: (a) vacancy at the center of nanowire (V_c), (b) vacancy at the edge of nanowire (V_e). Letters A, B, and C represent three substitution sites.

To further study the vacancy effect on the doping of SiNWs, the electronic structures of B-doped and P-doped SiNWs with vacancies are investigated respectively. Figure 5 shows the band structures of B-vacancy complexes in SiNWs. In the V_c configuration (see Fig. 5(a)), the formed B-vacancy complex induces the p-type feature of SiNWs but the acceptor level is deep and localized with respect to the B-doped perfect SiNWs. The calculated charge density indicates that the acceptor level mainly originates from the 2p states of the neighboring Si atoms of vacancy and the 2s states of B dopant atom. The result implies that the 2p electron of B impurity is captured by the dangling bonds of neighboring Si atoms, which results in a deep acceptor level in the SiNW. Therefore, there needs to be a high activation energy to induce free hole carriers for the B-doped SiNW with a central vacancy. In the V_e configuration (see Fig. 5(b)), the B doping induces a typical p-type feature and the calculated band structures are very similar to that of B-doped perfect SiNW.[21] The calculated charge density indicates that the acceptor levels mainly arise from the contribution of electronic states of B dopant and its neighboring Si atoms. The result suggests that the edge vacancy has almost no effect on the p-type doping of SiNWs.

Table 1. Energy differences between B- (P)-doped Si nanowire at a given site and its corresponding ground states in the V_c and V_e configurations.

Configuration			ΔE/meV	
			V_c	V_e
Dopant	B	Site A	177	148
		Site B	0	561
		Site C	63	0
	P	Site A	0	86
		Site B	329	0
		Site C	685	66

Figure 6 shows the band structures of P-doped SiNWs with Si vacancies. Compared with the band structure of V_c configuration, the P–V_c complex induces an obvious downshift of two mid-gap states (see Fig. 6(a)): the occupied state lies at the VBM and the unoccupied stays at the Fermi level. The result of charge-density indicates that the unoccupied mid-gap states originate from the 2p states of P dopant and its neighboring Si atoms. Moreover, the electronic states are very localized. The result suggests that the electrons of P-dopant are captured by the dangling bonds of the neighboring Si atoms, which results in the failure of n-type doping in SiNWs. In the V_e configuration (see Fig. 6(b)), the P doping induces a typical n-type feature. However, the donor level is 0.379 eV lower than CBM and it slightly deeper than that of P-doped perfect SiNWs.[15] From the partial charge-density, the main contribution of the donor level comes from the 2p electrons of P and its surrounding Si atoms. Moreover, the electronic states of the donor level are extended, thus the n-type doping of SiNWs is not significantly affected by the edge vacancy. The above results suggest that the vacancy, especially the vacancy located at the core region of SiNW, is a foundational obstacle for the n-type doping of SiNW.

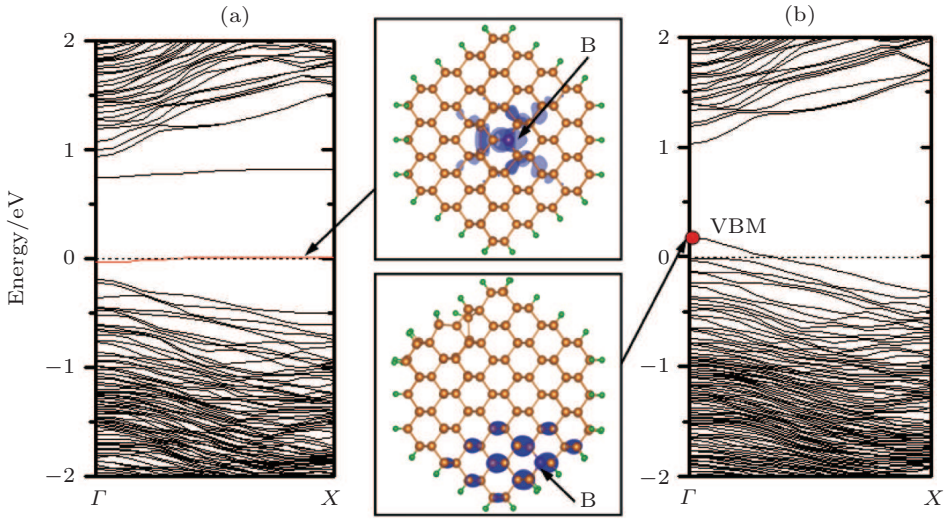


Fig. 5. (color online) Band structures of (a) B–V_c complex and (b) B–V_e complex in H-passivated SiNWs. The illustrations are the spatial distributions of charge-density for the partially occupied orbits in the V_c configuration and that of VBM at Γ point in the V_e configuration.

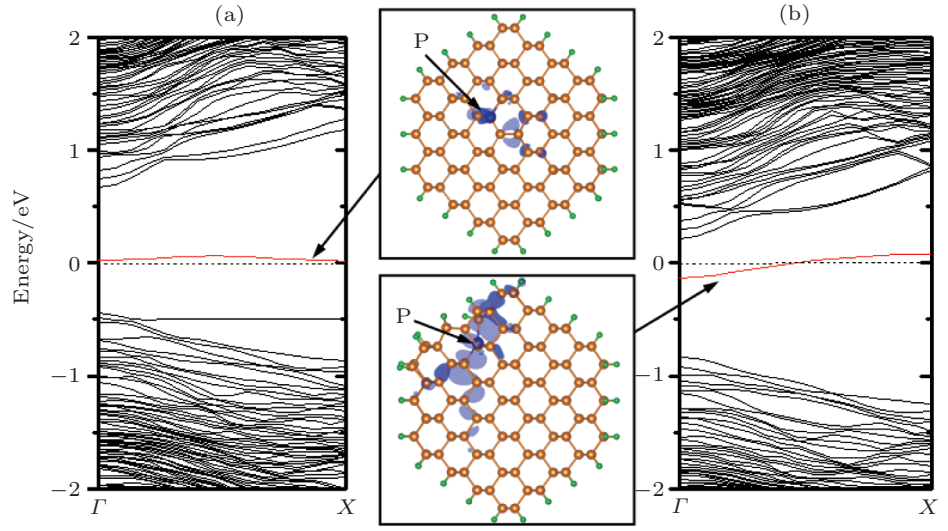


Fig. 6. (color online) Band structures of (a) P–V_c complex and (b) P–V_e complex in hydrogenated SiNWs. The illustrations are the spatial distributions of charge-density for the partially occupied orbit in the V_c configuration and that of VBM at Γ point in the V_e configuration.

4. Summary

In this paper, the stability of the Si vacancy and its effects on p-type and n-type dopings in H-passivated SiNW are investigated systematically based on the first-principles calculation. The vacancy located at the inner region of the nanowire (V_c) can be kept, while the vacancy at the edge of the nanowire (V_e) is excluded out of the nanowire due to local surface reconstruction. The results of formation energies suggest that the dopant atoms (B and P) can be trapped by the vacancy to form V_{Si}–B (V_{Si}–P) complex in the V_c configuration, while the V_e has little limit to the B and P dopings of SiNW. The further analysis of electronic structures indicates that B-doped SiNW can keep its p-type feature in the two vacancy configurations, but P-doped SiNW will lose its n-type feature when the central vacancy is introduced into SiNW. The results are in good agreement with experimental observations where the electric conductivity of n-type SiNW is generally lower than that of p-type SiNW.

Acknowledgment

The authors thank the Tianjin Supercomputer Center for supplying the computer resources.

References

[1] Lei L, Xu Q F , Hu M L, Sun H, Xiang G H and Zhou L B 2012 *Acta Phys. Sin.* **62** 037301 (in Chinese)

[2] Song Z M, Zhao D X, Guo Z, Li B H, Zhang Z Z and Shen D Z 2011 *Acta Phys. Sin.* **61** 052901 (in Chinese)

[3] Lu W, Mu Y M, Liu X Q, Chen X S, Wan M F, Shi G L, Qiao Y M, Shen S C, Fu Y and Willander M 1998 *Phys. Rev. B* **57** 9787

[4] Goldberger J, Hochbaum A I, Fan R and Yang P D 2006 *Nano Lett.* **6** 973
[5] Garnett E C and Yang P D 2008 *J. Am. Chem. Soc.* **130** 9224
[6] Garnett E C and Yang P D 2010 *Nano Lett.* **10** 1082
[7] Zhou X T, Hu J Q, Li C P, Ma D D D, Lee C S and Lee S T 2003 *Chem. Phys. Lett.* **369** 220
[8] Patolsky F, Zheng G F and Lieber C M 2006 *Nat. Protoc.* **1** 1711
[9] Xing Y J, Yu D P, Xi Z H and Xue Z Q 2002 *Chin. Phys.* **11** 1047
[10] Wu Y, Cui Y, Huynh L, Barrelet C J, Bell D C and Lieber C M 2004 *Nano Lett.* **4** 433
[11] Cui Y, Duan X F, Hu J T and Lieber C M 2000 *J. Phys. Chem. B* **104** 5213
[12] Wang Y F, Lew K K, Ho T T, Pan L, Novak S W, Dickey E C, Redwing J M and Mayer T S 2005 *Nano Lett.* **5** 2139
[13] Zheng G, Lu W, Jin S and Lieber C M 2004 *Adv. Mater.* **16** 1890
[14] Hong K H, Kim J, Lee J H, Shin J and Chung U I 2010 *Nano Lett.* **10** 1671
[15] Peelaers H, Partoens B and Peeters F M 2006 *Nano Lett.* **6** 2781
[16] Ko Y J, Shin M, Lee S and Park K W 2000 *J. Appl. Phys.* **89** 2001
[17] Kresse G and Furthmüller J 1996 *Comp. Mater. Sci.* **6** 15
[18] Perdew J P, Burke K and Wang Y 1996 *Phys. Rev. B* **54** 16533
[19] Ekardt W 1984 *Phys. Rev. B* **29** 1558
[20] Shu H B, Chen X S, Ding Z L, Dong R B and Lu W 2011 *J. Phys. Chem. C* **115** 14449
[21] Durgun E, Akman N, Ataca C and Ciracl S 2007 *Phys. Rev. B* **76** 245323